Characterization of Individual Threading Dislocations in GaN Using Ballistic Electron Emission Microscopy

H.-J. Im, Y. Ding, and J. P. Pelz
Department of Physics, The Ohio State University, Columbus, Ohio 43210

B. Heying and J. S. Speck
Materials Department, University of California, Santa Barbara, California 93109
(Received 28 March 2001; published 20 August 2001)

Threading dislocations (TDs) of molecular beam epitaxy grown GaN film were studied with ultrahigh vacuum ballistic electron emission microscopy in order to quantify any fixed negative charge at identifiable TDs, with ~3 nm spatial and ~10 meV local barrier resolution. In contrast to several prior studies, we find no indication of fixed negative dislocation charge at specific TD structures, with a conservative upper limit of ~0.25 e^- per c-axis unit cell. We do observe evidence of *positive* surface charge at TDs and at GaN step edges, which may be due to local piezoelectric fields.

DOI: 10.1103/PhysRevLett.87.106802 PACS numbers: 71.55.Eq, 68.37.Ef, 73.40.Ns

GaN and its related alloys have received much attention in recent years for their proven and potential ability in optical and high power microwave device applications [1]. However, due to the lack of a suitable lattice-matched bulk substrate, they are usually grown on Al_2O_3 or SiC substrates with a high density of threading dislocations (TDs) and other defects [2]. These TDs in III-nitride films are thought to be electrically active and of major concern for electronic and optical device applications [2]. Recent calculations [3] and modeling of measured electron mobility [4,5] in GaN films grown by metal-organic chemical vapor deposition (MOCVD) suggested that TDs in the III-nitrides might develop a significant trapped negative charge density λ (up to 1 e^-/c, where e^- is the electronic charge and $c \cong 0.52$ nm is the c-axis lattice constant), due to defect levels located along or close to the dislocation core. Furthermore, recent studies done using scanning capacitance microscopy (SCM) (with ~50–100 nm resolution) on MOCVD GaN [6] and AlGaN/GaN films [7] gave qualitative [6] or semiquantitative [7] evidence of negative charge in regions ~100 nm across which appeared to be correlated with TD-induced "pits" on a bare surface [6]. An estimate $\lambda \approx 0.5$ e^-/c was made [7] by assuming planar geometry for the trapped charge and an effective SCM probe area of ~500 nm^2. It would clearly be desirable to make more quantitative measurements of dislocation charge with higher spatial resolution, in order to correlate any dislocation charge with specific types of TDs (e.g., edge, screw, or mixed type) and with film growth and processing conditions.

Here we report high-resolution observation and quantification of the charge along isolated, identifiable TDs near metal/GaN interfaces on molecular beam epitaxy (MBE) grown GaN using ultrahigh vacuum (UHV) ballistic electron emission microscopy (BEEM) [8], in conjunction with electrostatic modeling of the local potential profile close to a charged TD. BEEM can image and quantify trapped charge in wide band gap materials with high sensitivity and a few nm spatial resolution [9], since trapped negative charge produces a quantifiable increase in the local Schottky barrier height (SBH) and subsequent decrease in the local transmitted BEEM current. Surprisingly, our measurements *do not* show significant negative charge at TDs in our MBE-grown GaN films. Rather, we generally observe a small *decrease* in the local SBH and a small *increase* in the local BEEM current, consistent with local *positive* charge. Since we observed similar effects close to steps at the metal/GaN interface, we propose this may be due to piezoelectric effects and local stress variation at TDs and interface steps.

The GaN samples were grown at the University of California, Santa Barbara, and consisted of a 0.5 μm thick MBE grown Ga-face GaN(0001) film grown on a 1–2 μm thick MOCVD-grown GaN film on a sapphire substrate. The MBE epilayer was n doped using Si with a concentration of $N_D = 1 \times 10^{17}$ cm^{-3} (corresponding Debye length $L_D \cong 11$ nm), while the MOCVD buffer layer was unintentionally n doped. Prior to the BEEM studies at The Ohio State University, samples were successively cleaned in trichloro-ethylene, acetone, and methanol, followed by ammonium hydroxide etching and nitrogen blow-dry. Ohmic contacts were made using In solder on two corners of roughly square (~5 mm)^2 samples. Samples were then introduced into our custom-built UHV STM/BEEM system (base pressure ~1×10^{-10} Torr) [9], mildly outgassed ($< \sim 230\,^\circ$C) overnight, and then ~12 separate 0.5 mm-diameter Schottky diodes were made by depositing 6 nm thick Pt film at room temperature using e-beam evaporation. Samples were then passed into an adjacent UHV analysis chamber, where diode current-voltage (I-V) and nm-scale STM/BEEM measurements were performed *in situ* at room temperature.

The macroscopic I-V curves of the fabricated Pt/GaN Schottky diodes exhibited a range of behaviors, ranging from nearly Ohmic to highly rectifying. The most rectifying diodes were chosen for detailed STM/BEEM study,

 0031-9007/01/87(10)/106802(4)$15.00 © 2001 The American Physical Society

and typically had macroscopic SBH $\phi_{\mathrm{macro}} \cong 0.8$ eV and ideality factor $n \cong 1.4$ as determined from the measured diode I-V curves. Figure 1 shows a (750 nm)^2 image of the typical STM topography of the top surface of the 6 nm thick Pt film. On a large scale we can clearly see the step structure of the underlying GaN film that was present before the Pt film was deposited. At a much smaller scale we observe the ~5 nm nodular surface structure of the polycrystalline Pt film (see also Figs. 2–4). The regular step train of the GaN film is occasionally disturbed by characteristic step structures, such as the V-shaped or "wing" structures (Figs. 1 and 4), growth spirals (Figs. 2 and 3), and more rarely deeper extended pits and step-bunched "cliff" structures (not shown). These step structures were formed during growth of the MBE GaN film, as advancing step edges interact with local pinning sites at the GaN surface. Growth spirals such as that in Fig. 2 are well known from previous studies [10], and result from step growth around an isolated TD with a screw component. The wing structures are the most common ($\sim 10^8$–10^9 cm^2) and are observed in areas with a higher local miscut. They are most likely related to TDs, which exist at similar density in similar GaN films [10]. Those TDs were reported to be a combination of edge, screw, and mixed type TDs [10]. We note that TDs with a screw component should *terminate* surface steps. We have found that ~30% of the wing structures we have studied in detail do in fact bound more steps from one side of the wing than the other, indicating that they have a screw component.

We now present detailed, high-resolution STM/BEEM measurements of the isolated TD core area shown in Fig. 2 that we know must have a screw component. Figure 2(a) shows a (350 nm)^2 STM image of the Pt surface over this TD, showing the ~5 nm diameter Pt crystallites over two spiraling steps in the underlying GaN film. The TD terminates two steps since GaN film has a wurtzite structure with a two-layer (*ABAB*) stacking sequence. Figure 2(b) shows the simultaneously measured BEEM image [8,9] of the same area, i.e., a plot of the magnitude of the hot-electron current that is injected *over* the local Schottky barrier as a function of the tip position. As mentioned above, significant trapped negative charge at the TD core should *reduce* the local BEEM current I_c, producing a "dark spot" in the BEEM image [9]. In contrast, we actually observe a modest *enhancement* (~40%) of I_c at the TD core. We also see a similar enhancement along the two spiraling step edges emanating from the TD core. The finer scale contrast in Fig. 2(b) is typical of BEEM images, and is mostly due to the spatially varying thickness of the metal film as well as the ~20 fA current noise in our BEEM system.

We next measured the variation of the local SBH around the TD, which can be directly related to fixed charge through electrostatic modeling [9]. Figure 3 shows a close-up (50 nm)^2 scan over the TD core area. This region was scanned 22 times, with the scan center adjusted after each scan to compensate for the ~1 nm drift between images. During each scan, the STM tip was stopped for ~20 s at each of the positions marked by a "×" symbol in Figs. 3(a) and 3(b), where an individual BEEM I-V curve [8,9] was measured in order to extract the local SBH ϕ_B. The spectra from the corresponding location in the 22 scans were then averaged together to yield a low noise ($< \sim 10$ meV) high spatial resolution ($< \sim 3$ nm) profile of ϕ_B across the TD core. Figure 3(c) plots a typical averaged BEEM I-V. This SBH profile is shown in Fig. 3(d), while the corresponding profile of I_c is shown in Fig. 3(e). The SBH profile shows only a small variation (~100 meV) that is roughly anticorrelated with the I_c profile. Also, the SBH is *decreased* near the TD core and the profile is not symmetric with respect to the core. In contrast, one would expect an *increased* SBH with roughly symmetric radial profile around a negatively charged TD.

Since the wing structures are more common in our samples than the growth spirals, we have also performed similar high-resolution studies across the core region of several wing structures. Figure 4 shows the results of one such study, measured in a similar way as Fig. 3. Our

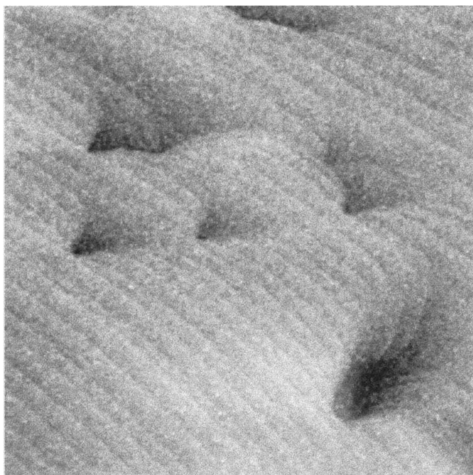

FIG. 1. (750 nm)^2 STM topography of 6 nm-Pt coated GaN. Tip bias $V_T = -1.6$ V and tunnel current $I_T = 4$ nA. Gray scale is ~10 nm. The wing structures are likely related to TDs (see text).

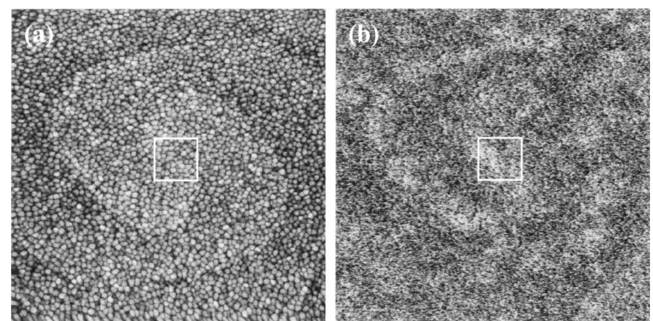

FIG. 2. (a) (350 nm)^2 STM topography and (b) corresponding BEEM image around a growth spiral ($V_T = -1.4$ V, $I_T = 4$ nA). Gray scales: (a) ~10 nm, (b) 1 pA. Square boxes indicate where detailed close-up study (Fig. 3) was done.

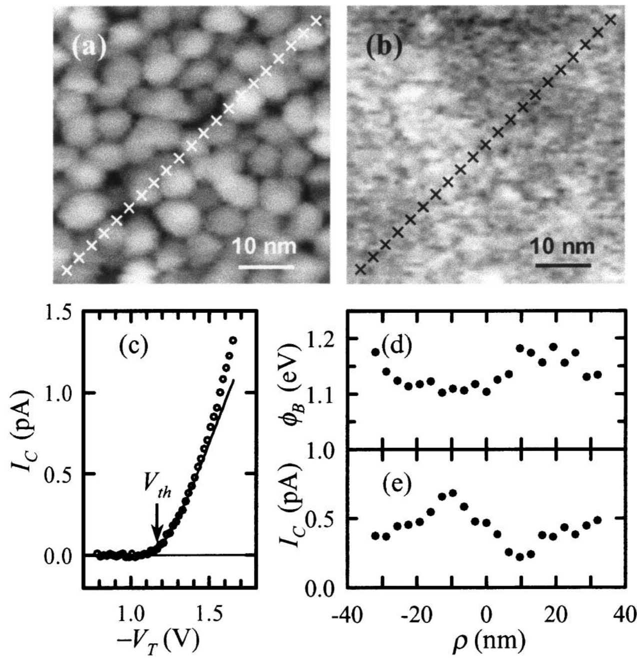

FIG. 3. (a) $(50\ \mathrm{nm})^2$ STM topography and (b) BEEM image at TD core region ($V_T = -1.4$ V, $I_T = 10$ nA). 21 crosses mark where BEEM spectra were taken. (d),(e): Profiles across TD core of (d) ϕ_B and (e) I_c, with the TD core located at $\rho = 0$ ($\rho < 0$: lower left corner).

observations are essentially the same as for the growth spiral: a modest *decrease* in the SBH at the TD core area at the wing apex, roughly anticorrelated with an increased local I_c. We also performed a similar high-resolution profile across a 5-layer high cliff structure (not shown) and observed similar local decrease in ϕ_B and increase in I_c. In general, TD structures imaged in large-area $(\sim 1\ \mu\mathrm{m})^2$ BEEM images often show somewhat increased I_c, but never any significant reduction as would be expected from negative charge at a TD core. Most step edges also showed a similar local increase in I_c.

To quantify the expected change in ϕ_B from negatively charged TDs, we consider a model consisting of a series of fixed electrons (each with charge e^-) starting from the Pt/GaN interface, separated by an equal distance nc ($n = 1, 2, 3, \ldots$) along the c direction, and truncated at the depletion width ($\sim 9L_D$) below the Pt/GaN interface due to screening. We assume the Fermi level is pinned at 1.13 eV below the conduction band edge at the interface, with this Dirichlet boundary condition satisfied by appropriate image charges. We used the unscreened Coulomb potential with the GaN dielectric constant ($\epsilon_s/\epsilon_0 = 9$) since the free carrier density in the first half of the depletion region is so small ($< \sim 3 \times 10^{12}\ \mathrm{cm}^{-3}$) as to produce negligible screening within 50 nm of the TD core. The solid curves in Figs. 5(a) and 5(b) show the calculated potential barrier maximum ϕ_B *projected* onto the metal/GaN interface as a function of radial distance ρ from the TD core for the cases of $n = 2$ and 3, respectively. These curves represent the minimum energy necessary for an electron injected a distance of ρ away from the TD core to overcome the potential barrier, if it followed a straight-line path normal to the interface. In reality, electrostatic repulsion would deflect the electron *sideways* slightly away from the TD through regions with lower potential, and might allow slightly lower energy electrons to enter the GaN substrate and be collected as BEEM current. To calculate this lower "effective" SBH ϕ_B^{eff}, we have calculated semiclassical trajectories [11] of hot electrons injected a distance ρ from the TD, to determine the minimum electron energy necessary to enter the GaN substrate. This is shown in the dashed lines in Figs. 5(a) and 5(b). We see that ϕ_B^{eff} is somewhat lower than the projected ϕ_B, but still exhibits a significant increase within a 5–8 nm radius from the TD core.

One conclusion from Fig. 5 is that any significant negative charge close to the TD core should have been observed as an increased local barrier. Specifically, barrier increases of $> \sim 200$ meV or $> \sim 100$ meV are expected within ~ 3 nm radius for $\lambda = e^-/2c$ and $e^-/3c$, respectively, well within the resolution of our measurements. Figure 5

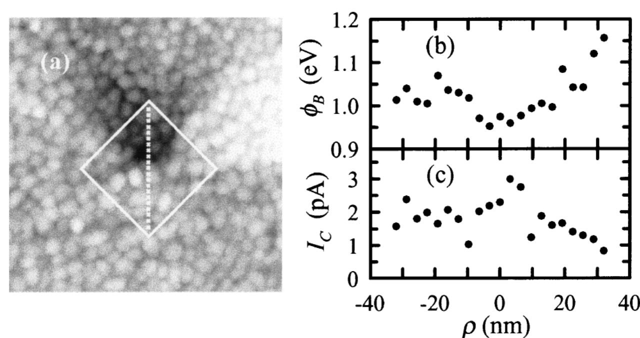

FIG. 4. (a) STM topography ($V_T = -1.6$ V, $I_T = 10$ nA) of a typical wing structure. Potential profiling was performed along 21 crosses in the $(50\ \mathrm{nm})^2$ box. (b),(c): Profiles of (b) ϕ_B and (c) I_c, with the TD core located at $\rho = 0$ ($\rho < 0$: lower corner).

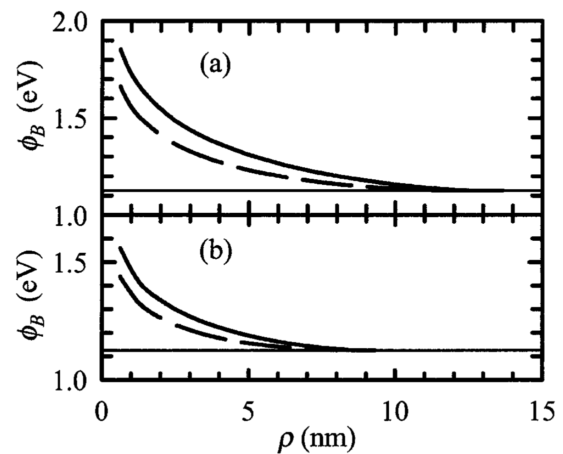

FIG. 5. Calculated profiles of ϕ_B (solid lines) and ϕ_B^{eff} (dashed lines) (see text) for (a) $\lambda = e^-/2c$ and (b) $\lambda = e^-/3c$. Horizontal solid lines at 1.13 eV represent the average SBH.

also indicates that there should be a significant *suppression* of the BEEM current close to the TD core, which would appear as a darker region in BEEM images such as Figs. 2(b) and 3(b). For example, at the tip bias of -1.4 V [as in Figs. 2(b) and 3(b)], there would be a black spot (with zero BEEM current) of diameter >4.5 and 1.6 nm for $\lambda = e^-/2c$ and $e^-/3c$, respectively, and a larger dark spot (with reduced BEEM current) of diameter $\sim$10 and 6 nm, respectively [9]. In fact, the observed BEEM images show neither a black spot nor a dark region of suppressed BEEM current close to the TD core area. We place a conservative limit of λ to be smaller than $e^-/4c$ at TDs in our MBE GaN films.

Although our observations appear inconsistent with previous measurements suggesting substantial negative charge at TDs [3–7], we note several differences in our samples and measurement technique. (1) We used MBE GaN films, grown under Ga rich conditions, while the samples used in other studies were grown by MOCVD. It is possible that the trapping characteristics of TDs may depend strongly on growth conditions. For example, the amount of excess near-surface Ga or N could be affected by growth and/or processing conditions [12], which in turn could affect the local charge trapping behavior close to TDs. (2) For a one-dimensional trapped charge configuration (e.g., charges along a TD), charges located close (within $\sim$50 nm) to the metal/GaN interface have a stronger effect on the effective SBH measured by BEEM than charges located deeper in the bulk. If near-interface traps along a TD are somehow *passivated* (e.g., by Pt), then the resulting effective barrier due to the remaining deeper charges might be missed in BEEM measurements. On a related note, if TD-related traps all happen to be located within $\sim$1 eV of the GaN conduction band minimum, then band bending in the depletion region would naturally empty near-interface traps, resulting in a smaller local effective barrier increase. We are presently planning experiments to test these possibilities.

As noted above, we generally observe a moderate decrease in ϕ_B and correlated increase in I_c at *both* TD structures and at step edges. Since nonuniform stress fields are present at both TDs and at steps, we suggest that the observed variation in ϕ_B and I_c may be due to the large piezoelectric effects associated with the GaN and AlGaN [13]. In particular, we note that the asymmetric profile in ϕ_B and I_c across the TD in Fig. 3 is reminiscent of dipolelike polarization fields that are expected at TDs with an edge component [13]. Finally, we note that a BEEM study by Brazel *et al.* [14] also reported enhanced I_c and reduced BEEM threshold at pits thought to be related to TDs, but that their measurements differ from ours in several significant qualitative ways that make direct comparison difficult. In particular, (1) they observe zero BEEM current everywhere except at certain surface pits (while we observe rather uniform BEEM current everywhere including at TDs); (2) when they do see BEEM, the threshold has a diodelike *exponential* turn-on (for both electron and hole injection) growing to a huge local current ($\sim$50% of the tunnel current), rather than the expected power-law form [8] only for electron injection, as shown in Fig. 3(c).

In summary we used BEEM to quantify possible charge at individual TDs in MBE grown GaN with nm-scale resolution. Contrary to previous reports, we see no evidence of significant fixed negative TD charge close to the metal/GaN interface, with an estimated upper limit of charge density $e^-/4c$. Rather, we see evidence of a small positive surface charge at TDs and at GaN step edges that might be due to local strain-related piezoelectric fields.

The authors thank E. T. Yu and E. R. Heller for helpful remarks. The work at the OSU was supported by the Office of Naval Research under Grant No. N00014-93-1-0607 (Dr. Colin Wood). The work at UCSB was supported by the ONR through the POLARIS MURI (Dr. Colin Wood, program manager).

[1] S. Nakamura, T. Mukai, and M. Senoh, Appl. Phys. Lett. **64**, 1687 (1994); Q. Chen *et al.,* IEEE Trans. Electron Devices **19**, 44 (1998).
[2] S. D. Lester, F. A. Ponce, M. G. Craford, and D. A. Steigerwald, Appl. Phys. Lett. **66**, 1249 (1995); J. S. Speck and S. J. Rosner, Physica (Amsterdam) **273B/274B**, 24 (1999).
[3] D. C. Look and J. R. Sizelove, Phys. Rev. Lett. **82**, 1237 (1999).
[4] K. Leung, A. F. Wright, and E. B. Stechel, Appl. Phys. Lett. **74**, 2495 (1999).
[5] H. M. Ng *et al.,* Appl. Phys. Lett. **73**, 821 (1998).
[6] P. J. Hansen *et al.,* Appl. Phys. Lett. **72**, 2247 (1998).
[7] D. M. Schaadt, E. J. Miller, E. T. Yu, and J. M. Redwing, Appl. Phys. Lett. **78**, 88 (2001).
[8] W. J. Kaiser and L. D. Bell, Phys. Rev. Lett. **60**, 1406 (1988); L. D. Bell and W. J. Kaiser, *ibid.* **61**, 2368 (1988).
[9] B. Kaczer, Z. Meng, and J. P. Pelz, Phys. Rev. Lett. **77**, 91 (1996); B. Kaczer, H.-J. Im, J. P. Pelz, and R. M. Wallace, Appl. Phys. Lett. **73**, 1871 (1998).
[10] B. Heying *et al.,* J. Appl. Phys. **85**, 6470 (1999); B. Heying *et al., ibid.* **88**, 1855 (2000).
[11] The trajectory of an electron wave packet propagating in GaN is calculated by numerically solving Newton's equation using conduction band effective mass and the force from the calculated potential gradient.
[12] V. M. Bermudez, D. D. Koleske, and A. E. Wickenden, Appl. Surf. Sci. **126**, 69 (1998).
[13] E. T. Yu *et al.,* Appl. Phys. Lett. **73**, 1880 (1998); C. Shi, P. M. Asbeck, and E. T. Yu, *ibid.* **74**, 573 (1999).
[14] E. G. Brazel, M. A. Chin, and V. Narayanamurti, Appl. Phys. Lett. **74**, 2367 (1999).